

# Non-unitary Entanglement Dynamics in Continuous Variable Systems

Tianci Zhou<sup>1,\*</sup> and Xiao Chen<sup>2,†</sup>

<sup>1</sup>*Kavli Institute for Theoretical Physics, University of California, Santa Barbara, CA 93106, USA*

<sup>2</sup>*Department of Physics, Boston College, Chestnut Hill, Massachusetts 02467, USA*

(Dated: March 1, 2025)

We construct random unitary Gaussian circuit for continuous-variable (CV) systems subject to Gaussian measurements. We show that when the measurement rate is nonzero, the steady state entanglement entropy saturates to an area-law scaling. This is different from many-body qubit system, where a generic entanglement transition is widely expected. The absence of entanglement phase transition is attributed to the diverging entangling time for the local degrees of freedom under unitary evolution, in contrast to the order one time to disentangle by local measurement. For the same reasoning, the absence of transition should also hold for other non-unitary Gaussian CV dynamics.

## I. INTRODUCTION

Recent years have seen a surge of interest in many-body non-unitary quantum dynamics from the perspective of quantum trajectories[1–15]. A simple toy model is a hybrid random circuit composed of both local unitary gate and projective measurement[2, 3, 6–8, 15]. The competition between the unitary dynamics and the local measurement leads to an entanglement phase transition of the steady state, separating the highly entangled volume law phase from the disentangled area law phase[3, 6–9]. This discovery leads to a series of developments and discoveries on non-unitary dynamics, such as the error correcting properties of the volume law phase[2, 11, 14, 15], the symmetry protected non-trivial area law phase[12, 13, 16] and the connection with the classical statistical mechanics models[4, 5, 17, 18].

In all these studies, the local degree of freedom is a qubit or a generalized qudit, which is discrete in nature and they are referred to as the discrete-variable (DV) systems. In contrast to this, many quantum systems are intrinsically continuous and are referred to as continuous-variable (CV) systems(see review [19]). These systems have infinite Hilbert space dimensions with the physical observables having a continuum of eigenvalues. Furthermore, these CV modes can be coupled together and form a many-body quantum system. In this paper, we build up a Gaussian many-body quantum circuit. In particular, we focus on the non-unitary random circuit models and explore the entanglement scaling of the Gaussian states.

Previously, Ref. 20 constructed a Gaussian random unitary circuit by using a set of fundamental one/two-mode CV gates and studied the information spreading and entanglement dynamics of the circuit. They found that analogous to the DV systems, there is a linear light cone for information spreading for systems with local interaction. After the local information reaches the bound-

ary of the system, the entanglement entropy scales linearly in the subsystem size. However, due to the infinite local Hilbert space dimension, the entanglement entropy of a subsystem is unbounded and continues to grow in time. This is different from the aforementioned DV system in which the local degree of freedom takes only  $O(1)$  time to reach equilibrium. Such a difference leads to a qualitative change of entanglement dynamics in the hybrid CV non-unitary dynamics. The unitary evolution takes an infinitely long time to entangle the local mode with the rest of the system and cannot compete with the Gaussian measurement which typically disentangles a single mode from the system in  $O(1)$  time. As a consequence, there is no entanglement transition in this model and a nonzero measurement rate drives the system to an area law phase. We verify this result numerically in a random Gaussian circuit subject to measurement and generalize this result to other non-unitary CV dynamics.

## II. ENTANGLEMENT DYNAMICS IN GAUSSIAN CV SYSTEMS

In this section, we briefly review the quantum information aspect of the continuous-variable systems. We mostly follow the convention of Ref. 21 with the exception that covariance matrices match  $\frac{1}{2}$  of the counterparts in Ref. 21.

A continuous-variable system is a quantum system that has operators with continuous spectrum. An  $L$ -mode harmonic oscillator system on lattice is a prototypical bosonic example. It has position and momentum operators with continuous spectrum, which are collectively denoted as  $X = [\mathbf{q}, \mathbf{p}]^T$  (the quadratures). The infinite dimensional Hilbert space can be constructed in the number basis, i.e. the simultaneous eigenstates of the number operators  $\prod_{i=1}^N a_i^\dagger a_i$ , where the mode creation/annihilation operators are related to the quadratures through

$$a_i = \frac{1}{\sqrt{2}}(q_i + ip_i) \quad a_i^\dagger = \frac{1}{\sqrt{2}}(q_i - ip_i) \quad (1)$$

\* tzhou@kitp.ucsb.edu

† chenaad@bc.edu

in the convention  $\hbar = 1$ . These operators have the canonical commutation relations

$$[X_i, X_j] = iJ_{ij}, \quad [a_i, a_j^\dagger] = \delta_{ij}, \quad (2)$$

where  $J$  is a  $2L \times 2L$  symplectic matrix

$$J = \begin{bmatrix} 0 & \mathbb{I} \\ -\mathbb{I} & 0 \end{bmatrix}. \quad (3)$$

Below we review elementary properties of the Gaussian states and Gaussian operations.

### A. Gaussian states and Gaussian operations

*Gaussian states* are defined by a Gaussian characteristic or Wigner function. For a pure state, the definition is equivalent to a Gaussian wavefunction in the quadrature (either position or momentum) basis. Its properties are therefore completely determined by the first two moments: the displacement vector  $\text{tr}(\rho X)$  and the covariance matrix

$$M_{ij} = \frac{1}{2} \text{tr}(\rho \{ (X_i - \langle X_i \rangle), (X_j - \langle X_j \rangle) \}), \quad (4)$$

where  $\{, \}$  denotes anti-commutator. In an  $L$ -mode system,  $M$  is a  $2L \times 2L$  real symmetric matrix satisfying the uncertainty principle  $2M \geq iJ$ . It can be “diagonalized” by a symplectic matrix  $S \in \text{Sp}(2N, \mathbb{R})$  into the Williamson normal form

$$M = S \text{diag}(\nu_1, \dots, \nu_N, \nu_1, \dots, \nu_N) S^\top \quad (5)$$

where  $\{\nu_i | i = 1, \dots, N\}$  are the  $N$  (non-negative) Williamson eigenvalues. The Rényi entanglement entropies of the Gaussian states only depend on the Williamson eigenvalues and are given by [21]

$$S_\alpha = \frac{\sum_{i=1}^N \ln[(\nu_i + \frac{1}{2})^\alpha - (\nu_i - \frac{1}{2})^\alpha]}{\alpha - 1}. \quad (6)$$

A special example is the 2nd Rényi entropy, which is

$$S_2 = \sum_{i=1}^N \ln 2\nu_i = \frac{1}{2} \ln \det(2M). \quad (7)$$

Due to its irrelevance to the entanglement, we set the displacement vectors to be zero afterwards.

*Gaussian operations* transform a Gaussian state to a Gaussian state. For instance, given a Gaussian initial state  $|\psi\rangle$ , a unitary evolution  $e^{-iHt}|\psi\rangle$  with Hamiltonian quadratic in the quadrature (or creation and annihilation operators) produces another Gaussian state, thus a Gaussian operation. Such unitary transformation preserves the commutation relation of the quadratures  $[\hat{U}^\dagger X_i \hat{U}, \hat{U}^\dagger X_j \hat{U}] = [X_i, X_j]$ . Infinitesimally, the transformation on the quadrature is linear, which generates a symplectic transformation for finite time:

$$\hat{U}^\dagger X \hat{U} = SX, \quad S \in \text{Sp}(2L, \mathbb{R}). \quad (8)$$

gate	$\hat{u}$	$S$
phase rotation	$\exp(i\theta a^\dagger a)$	$\begin{bmatrix} \cos \theta & \sin \theta \\ -\sin \theta & \cos \theta \end{bmatrix}$
one-mode squeezing	$\exp(\frac{1}{2}(ra^{\dagger 2} - ra^2))$	$\begin{bmatrix} e^r & 0 \\ 0 & e^{-r} \end{bmatrix}$
beam splitter	$\exp(\phi(a^\dagger b - ab^\dagger))$	$(\cos \phi \mathbb{I}_2 + i \sin \phi \sigma_y) \otimes \mathbb{I}_2$
two-mode squeezing	$\exp(r(a^\dagger b^\dagger - ab))$	$\cosh r \mathbb{I}_4 + \sinh r \sigma_z \otimes \sigma_x$

Table I. Unitary gates on one mode and two modes. The symplectic matrices are acting on the corresponding quadrature,  $[q_1, p_1]^\top$  for one mode and  $[q_1, p_1, q_2, p_2]^\top$  for two-mode.

Consequently the Gaussian property of the state is preserved, and the time evolved correlation matrix is given by

$$M(t) = SM(t=0)S^\top. \quad (9)$$

Examples of one-mode and two-mode evolutions are listed in Tab. I. We will use these operations as quantum unitary gates in the design of the circuit in Sec. III.

Furthermore, certain projective measurements are Gaussian operations. For example, a homodyne measurement corresponds to a projective measurement to quadrature basis  $|q\rangle$  or  $|p\rangle$  (infinitely squeezed states). It can produce a Gaussian state for the part of the system that is not measured. Projections to a coherent state  $|\alpha\rangle = D(\alpha)|0\rangle$  (a displaced Harmonic oscillator ground state) is called a heterodyne measurement. For pure states, since the wavefunctions are Gaussian, their overlaps with another Gaussian wavefunction are again Gaussian. Hence projective measurements to Gaussian states are Gaussian operations. Similar argument can be made to mixed state, in which we can first purify to a larger Gaussian state, then take the projective measurement and finally trace out the environment.

Finally, imaginary time evolution as a weak form of projective measurement is also a Gaussian operation. That means the normalized state under an imaginary time evolution of a quadratic Hamiltonian  $H$

$$\frac{e^{-\beta H}|\psi\rangle}{\langle\psi|e^{-2\beta H}|\psi\rangle} \quad (10)$$

is a Gaussian state if the original state  $|\psi\rangle$  is (see an operational proof in App. A).

In Sec. III, we will construct an  $L$ -mode hybrid quantum circuit model by applying a sequence of one-mode and two-mode Gaussian gates introduced in this section.

### B. Entanglement for Two-mode System

Qubit systems have a finite local Hilbert space, and entanglement of a finite spatial region has a saturation value upper bounded by the logarithm of the Hilbert

space dimension. This is not the case for a CV system. The infinite local Hilbert space gives rise to an unbounded entanglement growth, even for a two-mode system.

For example, starting from the vacuum state we repeatedly apply a two-mode squeezing gate with squeezing parameter  $r$  to obtain the state,

$$\begin{aligned} |\psi(t)\rangle &= [\exp(r(a^\dagger b^\dagger - ab))]^t |00\rangle \\ &= \frac{1}{\cosh rt} \sum_{n=0}^{\infty} (\tanh rt)^n |nn\rangle. \end{aligned} \quad (11)$$

The 2nd Rényi entropy for the subsystem of the first mode can be calculated from the covariance matrix  $M = \frac{1}{2}SS^\top$ . We have

$$S_2 = \ln \cosh 2rt \sim 2rt \text{ for large } rt. \quad (12)$$

The entanglement has an unbounded growth with an asymptotic linear time dependence.

This state has the property

$$\langle (q_1 - q_2)^2 \rangle = \langle (p_1 + p_2)^2 \rangle = e^{-rt}. \quad (13)$$

When  $rt$  is large, it is a very good practical approximation of the perfect EPR state with two photons at the same position and having almost opposite momentum

$$\delta(q_1 - q_2)\delta(p_1 + p_2). \quad (14)$$

### III. HYBRID GAUSSIAN CV CIRCUIT

In a qubit system, it is expected that there is a generic entanglement phase transition in the hybrid quantum circuit composed of both unitary evolution and projective measurements[2, 3, 6–8, 15]. When the measurement rate is small, there is a stable volume law phase. As we increase the measurement rate, there is a transition to the disentangled area law phase.

Inspired by the developments in the DV system, in this section, we construct a similar circuit for a CV system, see Fig. 1. We use independent random phase shift and one-mode squeezing to scramble the local Hilbert space and random beam splitter to entangle neighboring sites. The random parameter choices are uniform random  $\theta$  and  $\phi$  in  $[0, 2\pi]$  and uniform random squeezing parameter  $r \in [0, 1]$ , see explicit expressions in Tab. I. Then with probability  $p$ , we apply projective measurement to the single mode ground state  $|0\rangle$  on each site. The initial state is chosen as the tensor products of  $|0\rangle$ .

When  $p = 0$ , the circuit is completely unitary and has been studied by Ref. 20. In DV system with local interactions, the von Neumann entanglement entropy grows linearly in time and saturates to a volume law scaling[22]. The situation is quite different here in the CV setting. The entanglement entropy has an initial  $t^2$  growth, and then crossovers to a linear unbounded growth, see Fig. 2(a).

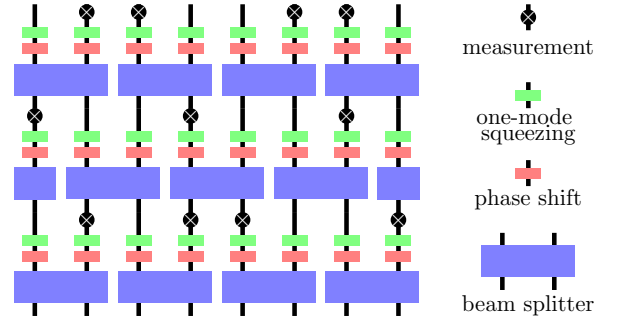


Figure 1. Structure of the hybrid circuit. Random one-mode squeezing and phase shift are used to scramble local Hilbert space, a random two-mode beam splitter is used to entangle nearby modes. Measurements to the vacuum state are inserted with rate  $p$ .

The entanglement can be estimated by computing the dimension of the effective Hilbert space. In a DV system, the maximal local Hilbert space dimension is fixed to be  $d$ . The locally interacting gate expands the domain of influence linearly. Hence the effective Hilbert space dimension along either side of the entanglement cut is roughly  $d^t$ . Taking logarithm gives a linear growth of the entropy. After the saturation time,  $t \sim L$ , the entanglement saturates to a volume law value. In a CV system, besides the linear spreading in the spatial direction, the explored local Hilbert space dimension  $d$  is also growing exponentially in time. Taking into account both effects gives a  $t^2$  growth at early time (see Fig. 2(a)). After the domain of influence reaches the whole system, the effective Hilbert space can continue to grow as  $d^L \sim e^{tL}$ . Taking logarithm gives rise to the late time linear  $t$  growth observed in Fig. 2(a).

When we turn on a projective measurement  $|0\rangle\langle 0|$  with finite rate of measurement  $p$  (see numerical algorithm in App. B), the entanglement growth is system size independent. It has a short time growth and eventually saturates to a system size independent value, i.e. an area law, see Fig. 2(b).

We replace the measurement by an imaginary single-mode gate. Operationally, we set  $p = 1$  (measuring all sites after the one-mode squeezing) and replace the measurement from the projection to  $|0\rangle$  to a weaker imaginary time evolution  $e^{-\beta a_i^\dagger a_i}$ . The tuning parameter is now  $\beta$ . We observe similar area law behavior in Fig. 2(c) when  $\beta$  is finite.

We believe that the infinite Hilbert space dimension plays the crucial role for the absence of the entanglement phase transition. For the sake of argument, assuming that the local Hilbert space dimension for the CV system is truncated at a finite but very large number  $K$ . It takes  $O(\ln K)$  time to explore the local Hilbert space and creates entanglement  $\ln K$ , whereas a single projective measurement can destroy this entanglement immediately. As  $K \rightarrow \infty$ , the time scale associated with the measurement that destroys the entanglement is much

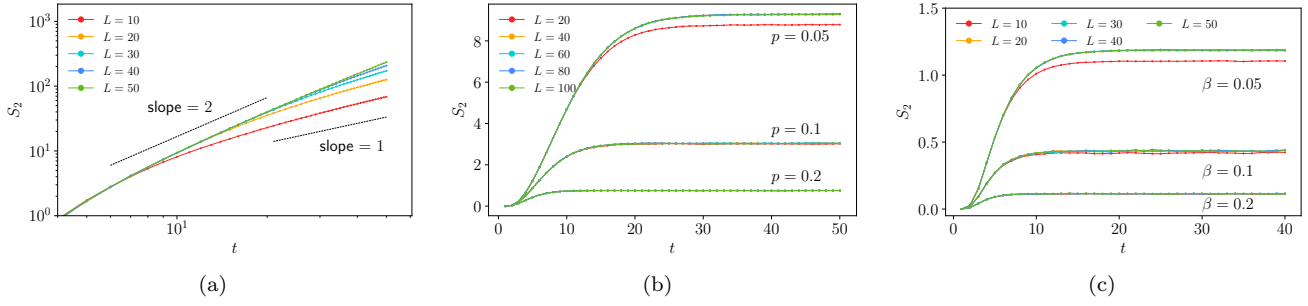


Figure 2. Averaged half system entanglement  $S_2$  in a hybrid circuit. Entanglement is averaged over random realizations of the gate. There are two circuit structures: either applying gates on odd bonds in the first step or on even bonds. The results here are the averages over equal probabilities of those two structures. (a) When the measurement probability  $p = 0$ , entanglement has a quadratic growth followed by a linear growth. (b) When  $p > 0$ , the averaged entanglement converges to system size independent values, with a slightly smaller saturation value when  $L \lesssim \frac{1}{p}$ . (c) We replace the projective measurement by imaginary evolution gate  $e^{-\beta \sum_i a_i^\dagger a_i}$ . We set  $p = 1$  and vary the strength parameter  $\beta$ . The entanglement converges to system size independent values.

smaller than the time scale to create entanglement, hence pushing the would-be transition probability  $p_c$  to 0.

### A. DV dynamics example

We can reproduce similar physics in a DV model with large local Hilbert space dimension. Consider a one dimensional qubit system with  $L$  sites. At each site, there is a cluster of  $N$  qubits. As shown in Fig. 3, in each time step, the unitary evolution involves both intra-cluster interaction and inter-cluster interaction. The intra-cluster interaction is realized by applying  $N/2$  two-qubit gates which randomly couples  $N/2$  pairs of qubits, while the inter-cluster interaction between neighboring two sites only has a *single* two-qubit gate. The projective measurement gate is applied at each site with probability  $p$  and can disentangle *every qubit* in one cluster.

The design of the interaction patterns ensure that there is roughly a  $\ln 2$  entanglement increase across the inter-cluster bond, until it reaches the maximal of  $N \ln 2$ . Hence it takes  $O(N)$  time for one cluster to get fully entangled with other clusters under unitary evolution. However, it takes only  $O(1)$  time<sup>1</sup> for one cluster to become disentangled under the projective measurement<sup>2</sup>. At finite  $N$ , the two time scales are still comparable, resulting in a phase transition at finite  $p_c$ . However,  $p_c$  will decrease with  $N$  and eventually vanishes when  $N \rightarrow \infty$ .

We numerically verify this idea in a random Clifford circuit and present the result in Fig. 4. This model

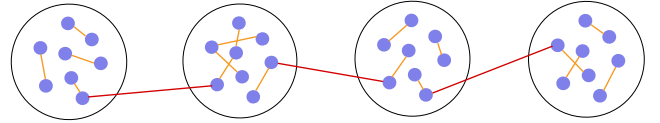


Figure 3. A cartoon picture for the qubit system. At each site, there are  $N$  qubits. The unitary dynamics at each time step involves two parts: (1) intra-site interaction described by the  $N/2$  two-qubit gates (denoted by the yellow line), (2) a single two-qubit gate connecting neighboring sites (red line).

can be efficiently simulated with a large number of qubits[23, 24]. We use the peak of the mutual information to identify the location of  $p_c$ [9]. As  $N$  increases,  $p_c$  moves to the left and approaches zero in the large  $N$  limit.

Notice that if we modify the unitary dynamics in Fig. 3 and introduce  $N$  two-qubit gates connecting neighboring sites, then the time scale to completely entangle two clusters reduces to  $O(1)$  and there is an entanglement phase transition at finite  $p_c$  [25], even after when sending  $N \rightarrow \infty$ .

## IV. CONCLUSION

In this paper, we study the entanglement dynamics in hybrid CV Gaussian circuits composed of both unitary and non-unitary gates. For a generic random unitary Gaussian dynamics, the entanglement entropy for a subsystem is proportional to the subsystem size and can grow indefinitely in time due to the unbounded local Hilbert space dimension. We show that this highly entangled phase is unstable when the system is subject to repeated Gaussian measurements. When the measurement rate is nonzero, the steady state evolves to an area law phase, indicating the absence of the entanglement

<sup>1</sup> This is comparable to the  $\ln K$  time scale (note  $K$  is the local Hilbert space dimension in the CV system) to entangle and  $O(1)$  time to disentangle in the CV case.

<sup>2</sup> In a Haar random circuit, the absence of the phase transition in the large  $N$  limit can also be understood in terms of the minimal cut picture[3].

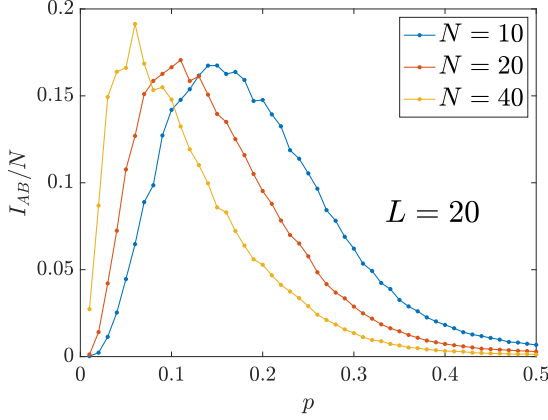


Figure 4. We consider a hybrid Clifford circuit composed of both unitary dynamics and projective measurement and compute the steady state mutual information  $I_{AB} = S_A + S_B - S_{AB}$  for various  $N$ . In each time step, the unitary dynamics is described by Fig. 3 with each bond denoting a random Clifford gate, and the projective measurement is applied randomly at each site with the probability  $p$ . After the measurement, all the qubits in one site are disentangled from the rest of system. At finite  $N$ , there is an entanglement phase transition with  $p_c$  characterized by the peak of  $I_{AB}$  of the steady state[9]. Here we consider periodic boundary condition and  $A$  and  $B$  are two antipodal regions with length  $L_A = L_B = 4$ .

transition.

We argue that the lack of phase transition is due to disparity of the competing time scales to entangle and disentangle the degrees of freedom. While it takes  $O(1)$  time scale to destroy the entanglement in a Gaussian measurement, it takes infinitely long time for a single mode to get entangled with the system. We reproduce this effect from a similar DV system construction with finite but large local Hilbert space dimension.

Our result holds for a generic Gaussian unitary circuit subject to Gaussian measurements and can be applied to other hybrid Gaussian dynamics, in which the Gaussian measurement is replaced by an imaginary evolution gate. We expect that our argument for the absence of the entanglement transition can be generalized to interacting hybrid CV dynamics. Moreover, it might be interesting to explore hybrid CV dynamics with extra constraints, such as the global  $U(1)$  symmetry, where an entanglement phase transition may exist. We leave this for the future study.

## ACKNOWLEDGMENTS

TZ was supported by a postdoctoral fellowship from the Gordon and Betty Moore Foundation, under the EPiQS initiative, Grant GBMF4304, at the Kavli Institute for Theoretical Physics. This research is supported in part by the National Science Foundation under Grant No. NSF PHY-1748958. We acknowledge sup-

port from the Center for Scientific Computing from the CNSI, MRL: an NSF MRSEC (DMR-1720256) and NSF CNS-1725797.

## Appendix A: Quadratic Imaginary Time Evolution is Gaussian

In this appendix, we show that the imaginary time evolution with a quadratic Hamiltonian is a Gaussian operation. Similar conclusion was proven for the fermionic case[26] by viewing Gaussian states as the limiting process of generalized canonical transformation. We here show that the imaginary time evolution can be decomposed as a series of Gaussian operations with the help of an auxiliary mode.

Let  $H$  be a quadratic Hermitian Hamiltonian, consider the state

$$\rho = e^{-\beta H} \rho_0 e^{-\beta H} / \text{tr}(e^{-2\beta H} \rho_0). \quad (\text{A1})$$

By Williamson theorem, the (non-negative) Hamiltonian can be diagonalized in a diagonal basis  $H = \sum_i \nu_i a_i^\dagger a_i$ .

We use a three-step process to engineer the operator  $e^{-\beta_i a_i^\dagger a_i}$ , where  $\beta_i = \beta \nu_i$ . First supplementing an environment state  $|0\rangle_0$ , then applying a two-mode squeezing operator on mode 0 (the environment) and mode  $i$ , finally making a projective measurement  $|0\rangle\langle 0|$  on mode 0. According to the disentangling identity[27]

$$\begin{aligned} \exp(r a_i^\dagger a_0^\dagger - r a_i a_0) &= \exp(\tanh r a_i^\dagger a_0^\dagger) \\ \exp(-\ln \cosh r (a_i^\dagger a_i + a_0^\dagger a_0 + 1)) &\exp(-\tanh r a_i a_0). \end{aligned} \quad (\text{A2})$$

Its action in these three steps is

$${}_0\langle 0| \exp(r a_i^\dagger a_0^\dagger - r a_i a_0) |0\rangle_0 \sim \exp(-\ln \cosh r a_i^\dagger a_i). \quad (\text{A3})$$

Therefore taking  $\ln \cosh r = \beta_i$  effectively creates the operator  $e^{-\beta_i a_i^\dagger a_i}$  acting on  $\rho_0$ . Since all these three steps are Gaussian, the operation  $e^{-\beta_i a_i^\dagger a_i}$  is Gaussian. Similarly we can repeat this process and create the imaginary time evolution on the other sites. Therefore the whole operation is Gaussian.

## Appendix B: Numerical Algorithms

In this appendix, we provide numerical formalisms to compute the change of the covariance matrix under a heterodyne measurement and a Gaussian non-unitary time evolution.

**Heterodyne measurement:** We rephrase the standard results from the review article [19] in our notation. It is best to carry out the commutation in a basis where the quadratures are ordered as  $[q_1, p_1, q_2, p_2, \dots, q_L, p_L]$ . Assuming the basis transformation through a  $T$  matrix

$$[q_1, p_1, q_2, p_2, \dots, q_L, p_L]^\top = T[\mathbf{q}, \mathbf{p}]^\top, \quad (\text{B1})$$



the covariance matrix in the new basis is

$$M_{qpqp} = TMT^\top = \begin{bmatrix} A & B \\ C & D \end{bmatrix}. \quad (\text{B2})$$

Here  $A, B, C, D$  are blocks of  $M_{qpqp}$  with size  $2(L-1) \times 2(L-1)$ ,  $2(L-1) \times 2$ ,  $2 \times 2(L-1)$ , and  $2 \times 2$  respectively. After a projective measurement to the ground state  $|0\rangle\langle 0|$  on the  $L$ th mode, the new covariant matrix  $M'_{qpqp}$  has a block structure

$$M'_{qpqp} = \begin{bmatrix} A' & B' \\ C' & D' \end{bmatrix}, \quad (\text{B3})$$

where the blocks are transformed as

$$\begin{aligned} A' &= A - C(-i\sigma_y)B(i\sigma_y) + \frac{1}{2}\mathbb{I}_2 C^\top \\ &\quad \times (\det(B) + \frac{1}{2}\text{tr}(B) + \frac{1}{4})^{-1} \\ B' &= C' = 0 \\ D' &= \frac{1}{2}\mathbb{I}_2. \end{aligned} \quad (\text{B4})$$

Then the new covariance matrix  $M'$  after measurement in the  $[\mathbf{q}, \mathbf{p}]$  basis is  $T^\top M'_{qpqp} T$ .

**Non-unitary time evolution:** we derive the equation of motion for the Gaussian state covariance matrix under a general non-unitary time evolution.

Specifically, let the Hamiltonian be quadratic

$$H = \frac{1}{2} X_i (F_{ij} - iG_{ij}) X_j, \quad (\text{B5})$$

where both  $F$  and  $G$  are real symmetric matrix. We seek

to find the equation of motion for

$$M_{ij}(t) = \frac{1}{2} \frac{\langle \psi | e^{iH^\dagger t} \{X_i, X_j\} e^{-iHt} | \psi \rangle}{\langle \psi | e^{iH^\dagger t} e^{-iHt} | \psi \rangle}. \quad (\text{B6})$$

By taking the time derivative and using the Wick theorem of the Gaussian states, we have

$$\partial_t M = -MFJ + JFM - 2MGM - \frac{1}{2}JGJ. \quad (\text{B7})$$

Setting  $G = 0$ , the equation of solely unitary evolution can be interpreted as a symplectic rotation. If we define a custom bracket

$$[F, M]_s = -MFJ + JFM, \quad (\text{B8})$$

then

$$\partial_t M = [F, M]_s, \quad (\text{B9})$$

whose solution is  $M(t) = SM S^\top$ , i.e. a rotation with the symplectic matrix  $S = \exp(JFt)$ .

When  $G$  is not equal to zero, we use the pure state condition  $MJM = \frac{1}{4}J$ [19] to reduce the equation of motion to

$$\partial_t M = [F + [M, G]_s, M]_s. \quad (\text{B10})$$

Thus infinitesimally it is still a symplectic rotation. The finite time evolution is a non-linear symplectic rotation  $M(t) = S(t)MS(t)^\top$ .

Numerically we use integration to solve the time dependent symplectic matrix  $S(t)$

$$\partial_t S(t) = J(F + [M, G]_s)S. \quad (\text{B11})$$

The algorithm uses the explicit 4th order Runge-Kutta scheme[28] followed by a Schultzs iteration[29] to preserve the symplectic feature of  $S(t)$ .

- 
- [1] Xiangyu Cao, Antoine Tilloy, and Andrea De Luca. Entanglement in a fermion chain under continuous monitoring. April 2018.
  - [2] Ruihua Fan, Sagar Vijay, Ashvin Vishwanath, and Yi-Zhuang You. Self-Organized Error Correction in Random Unitary Circuits with Measurement. *arXiv:2002.12385 [cond-mat, physics:quant-ph]*, February 2020.
  - [3] Brian Skinner, Jonathan Ruhman, and Adam Nahum. Measurement-Induced Phase Transitions in the Dynamics of Entanglement. *Physical Review X*, 9(3):031009, July 2019.
  - [4] Yimu Bao, Soonwon Choi, and Ehud Altman. Theory of the phase transition in random unitary circuits with measurements. *Physical Review B*, 101(10):104301, March 2020.
  - [5] Chao-Ming Jian, Bela Bauer, Anna Keselman, and Andreas W. W. Ludwig. Criticality and entanglement in non-unitary quantum circuits and tensor networks of non-interacting fermions. December 2020.
  - [6] Amos Chan, Rahul M. Nandkishore, Michael Pretko, and Graeme Smith. Unitary-projective entanglement dynamics. *Physical Review B*, 99(22):224307, June 2019.
  - [7] Yaodong Li, Xiao Chen, and Matthew P. A. Fisher. Quantum Zeno effect and the many-body entanglement transition. *Physical Review B*, 98(20):205136, November 2018.
  - [8] Michael J. Gullans and David A. Huse. Dynamical Purification Phase Transition Induced by Quantum Measurements. *Physical Review X*, 10(4):041020, October 2020.
  - [9] Yaodong Li, Xiao Chen, and Matthew P. A. Fisher. Measurement-driven entanglement transition in hybrid quantum circuits. *Physical Review B*, 100(13):134306, October 2019.
  - [10] Xiao Chen, Yaodong Li, Matthew P. A. Fisher, and Andrew Lucas. Emergent conformal symmetry in nonunitary random dynamics of free fermions. *Physical Review*

- Research*, 2(3):033017, July 2020.
- [11] Yaodong Li and Matthew P. A. Fisher. Statistical Mechanics of Quantum Error-Correcting Codes. *arXiv:2007.03822 [cond-mat, physics:quant-ph]*, July 2020.
  - [12] Ali Lavasani, Yahya Alavirad, and Maissam Barkeshli. Measurement-induced topological entanglement transitions in symmetric random quantum circuits. *arXiv:2004.07243 [cond-mat, physics:quant-ph]*, April 2020.
  - [13] Shengqi Sang and Timothy H. Hsieh. Measurement Protected Quantum Phases. *arXiv:2004.09509 [cond-mat, physics:quant-ph]*, April 2020.
  - [14] Michael J. Gullans, Stefan Krastanov, David A. Huse, Liang Jiang, and Steven T. Flammia. Quantum coding with low-depth random circuits. *arXiv:2010.09775 [cond-mat, physics:quant-ph]*, October 2020.
  - [15] Soonwon Choi, Yimu Bao, Xiao-Liang Qi, and Ehud Altman. Quantum error correction in scrambling dynamics and measurement-induced phase transition. *Physical Review Letters*, 125(3), Jul 2020.
  - [16] Matteo Ippoliti, Michael J. Gullans, Sarang Gopalakrishnan, David A. Huse, and Vedika Khemani. Entanglement phase transitions in measurement-only dynamics. *Physical Review X*, 11(1), Feb 2021.
  - [17] Adam Nahum, Jonathan Ruhman, Sagar Vijay, and Jeongwan Haah. Quantum Entanglement Growth under Random Unitary Dynamics. *Physical Review X*, 7(3):031016, July 2017.
  - [18] Tianci Zhou and Adam Nahum. Emergent statistical mechanics of entanglement in random unitary circuits. *Physical Review B*, 99(17):174205, May 2019.
  - [19] Christian Weedbrook, Stefano Pirandola, Raúl García-Patrón, Nicolas J. Cerf, Timothy C. Ralph, Jeffrey H. Shapiro, and Seth Lloyd. Gaussian quantum information. *Reviews of Modern Physics*, 84(2):621–669, May 2012.
  - [20] Quntao Zhuang, Thomas Schuster, Beni Yoshida, and Norman Y. Yao. Scrambling and complexity in phase space. *Physical Review A*, 99(6), Jun 2019.
  - [21] Gerardo Adesso, Sammy Ragy, and Antony R. Lee. Continuous Variable Quantum Information: Gaussian States and Beyond. *Open Systems & Information Dynamics*, 21(01n02):1440001, March 2014.
  - [22] Hyungwon Kim and David A. Huse. Ballistic spreading of entanglement in a diffusive nonintegrable system. *Physical Review Letters*, 111(12), Sep 2013.
  - [23] Daniel Gottesman. The heisenberg representation of quantum computers, 1998.
  - [24] Scott Aaronson and Daniel Gottesman. Improved simulation of stabilizer circuits. *Phys. Rev. A*, 70:052328, Nov 2004.
  - [25] Chunxiao Liu, Pengfei Zhang, and Xiao Chen. Non-unitary dynamics of sachdev-ye-kitaev chain, 2021.
  - [26] Sergey Bravyi. Lagrangian Representation for Fermionic Linear Optics. *Quantum Info. Comput.*, 5(3):216–238, May 2005.
  - [27] Ananda DasGupta. Disentanglement formulas: An alternative derivation and some applications to squeezed coherent states. *American Journal of Physics*, 64(11):1422–1427, November 1996.
  - [28] Desmond J. Higham. Time-stepping and preserving orthonormality. *BIT Numerical Mathematics*, 37(1):24–36, March 1997.
  - [29] Nicholas J. Higham, D. Steven Mackey, Niloufer Mackey, and Françoise Tisseur. Functions Preserving Matrix Groups and Iterations for the Matrix Square Root. *SIAM Journal on Matrix Analysis and Applications*, 26(3):849–877, January 2005.